

IMAGE-BASED AUTOMATIC TARGET RECOGNITION

Dr. Ram-Nandan P. Singh
Naval Air Systems Command
Patuxent River, MD 20670

Professor Mahmoud A. Abdullah
Manufacturing Engineering Department
Central State University
Wilberforce, Ohio 45384

A B S T R A C T

An image-based automatic target recognition (IATR) is basically a tactical decision aid that integrates all of the available information and produces a dynamic composite picture of a target for visualization and evaluation by an operator. In modern warfare, it has become an indispensable tool for precision strikes and surveillance missions of defense weapon systems. An IATR processes imagery data received from diverse imaging sensors for the purpose of target detection and recognition in real time. Using Wavelet Transforms, images are fused at different resolution levels to obtain a fused image. It has also been demonstrated that fusing the wavelet coefficient images directly can enhance the recognition contents of the image. This composite image contains all the information of interest for an IATR. In addition, an evaluation methodology based on visual perception and on statistical properties of the fused image is presented.

1.0 INTRODUCTION

In a fast technologically changing world of wireless communications, multi-spectral satellite imaging, space-based navigation, and internet networking, the Navy is transitioning its Global Command and Control Systems – Maritime (GCC-M) into PC-based Command and Control systems, and subsequently to web-based GCCS-M. The objective is that it will provide a **coherent, common tactical picture** to all members of a battle force across the theatre of operations in real time. An Image-based Automatic Target Recognition (IATR) will be one of the critical components of this new paradigm to achieve **total superiority** in any warfighting operation. Presently, multi-spectral satellite imagery and space intelligence are areas of increasing importance to the way we do business in battle. A platform equipped with an IATR will receive imagery from air, space, surface, and land; and be able to communicate with remote platforms. This will basically provide a powerful tool to warfighters for precision targeting using stand-off weapons.

Fusing imagery received from diverse sensors in real time is a highly challenging task. A fused product may provide a coherent and comprehensive tactical Situation Awareness

(SA). An information Fusion discipline seeks to provide a holistic approach to information analysis that addresses the inherent complexities of the SA problem. In this context, it is not just the information content (information measure) of a piece of data but also its relationship to other pieces of information that can be vital. Because the fusion products possess a multiple level-of-abstraction character, data fusion inherently requires a holistic level-of-abstraction approach to information combination. In general, the higher the level of command, the more abstract the required information fusion product.

An IATR is currently an active area of research. The IATR field has evolved from statistical pattern recognition approaches [6] to model-based vision and to knowledge-based systems. Also, adaptive and learning techniques focus on the part of the IATR problem only. Current research approaches to IATR include multi-resolution techniques, pyramid processing, neural nets, fuzzy logic, genetic algorithms, and random set theory [4, 10, 12, 13]. However, the image fusion techniques for image-based ATR are in an infancy state. References [1, 2] provide the state-of-the-art advancements in IATR technology.

Recently, a new trend in defense modernization industry has emerged. It easily realizes a multi-mission capability for a platform by adding more imaging sensors and data links. These multiple dissimilar image sensors provide spatial, temporal, spectral, polarimetric, and other observable characteristics of an image field, and combine high intelligibility with high contrast for interesting objects or phenomena. Some of these imaging sensors may be collocated, while the others may not. For an IATR, these image characteristics greatly enhance discrimination as well as tracking of targets including small and extended targets using shapes, size, color, temperature, spectral response, texture, and other attributes of these objects in imaged scenes.

The NAVY P-3C ASUW Improvement Program (AIP) has greatly embraced this trend. This program is making significant Pre-Planned Product Improvement (P3I) avionics upgrades to enhance ASUW, C4I, and OTH-T capabilities. Presently, the P-3C AIP aircraft imaging sensors include synthetic aperture radar (SAR)/ inverse synthetic aperture radar (ISAR), advanced imaging multi-spectral sensor (AIMS), Television camera, and missile warning systems. The AIMS system will eventually replace both the infrared detection system (IRDS) and E-O Sensor (EOS) currently installed on baseline AIP aircraft. Next, the goal for the P-3C AIP is to develop an ATR capability using these image sensors. This sets the motivation to develop an image-based automatic target recognition.

A three-phase development approach has been adopted for this project, namely, IATR-Part-I (Data Processing), IATR-II (Architecture Development), and IATR-III (Performance Evaluation). This paper presents IATR(Part-I) that fuses imagery received from multiple diverse sensors for target detection and recognition. These non-coherent and coherent imaging sensors include Electro-Optical sensors (EOS) and SAR radars. Also, because the individual imaging sensors on a single payload (multi-spectral satellite) are optically-aligned sensors, these diverse imagery data are self-registered. This, in turn, requires fusing multi-spectral imagery from multiple bands with space intelligence

for target recognition. IATR-II poses a technical challenge for research in the area of the DOD's Joint Technical Architecture (JTA). It aims at developing a common operational architecture with common operating pictures. Affordability and interoperability are the two factors that play important roles in its design. This architecture must be **truly flexible** that can easily accommodate new sensors and emerging technologies when they mature for applications. IATR-III will objectively and quantitatively evaluate IATR performance. This will apply an image metrics, and several MOPs. These will include a probability of detection (Pd), false alarm rates (FARs), and a confusion matrix. A confusion matrix represents the fraction of time that one target is mistaken for another.

This paper presents preliminary results on IATR (Part-I: Data Processing). It fuses images received from diverse sensors for the purpose of target detection and recognition. Using Wavelet Transforms, images are fused at different resolution levels to obtain a fused image. It has also been demonstrated that fusing the wavelet coefficient images directly can enhance the recognition contents of the image. This composite image contains all the information of interest for an IATR. In addition, it presents an evaluation methodology based on visual perception and on statistical properties of the fused images.

2.0 IMAGE FUSION

Fusion of images collected by several sensors has received wide acceptance as a mean of information condensation for reliable decision making. Using Wavelet Transforms, images are fused at different levels of resolution to obtain a final fused image that contains all the information of interest. It has been the experience that the wavelet transform accentuates the noise that corrupts the original images[16]. This paper compares the fusion of images directly using the raw images and using their wavelet transform. The comparison is based on the visual perception and on the statistical properties of the fused images.

Image fusion refers to the integration of the complementary information provided by several imaging sensors for greater object/target visibility and subsequent detection. Applications of image fusion are numerous and range from medical imaging to satellite mapping. As a prerequisite for image fusion, images from different sensors must be registered and with similar resolution. Many studies addressed the problem of image registration and resolution matching [3, 8, 9]. Also, a passive, multi-spectral imaging Electro-Optical(E-O) and Infrared (IR) sensor suite is able to collect imagery in several distinct wavelengths from the ultraviolet (UV) through the long wave infrared (LWIR). This single payload provides near-simultaneous multi-spectral, co-registered imagery of ground targets and background signatures. For a multi-spectral sensor, one of the IATR techniques is to fuse multiple wavebands into a single waveband. Then, apply some discrimination algorithms to classify the scene based on temporal variations of spectral signatures. Reference 18 discusses various approaches to discriminate targets from clutter in SAR imagery.

Image fusion can be performed using the raw images provided by the sensors or on different transformations of the images. Pyramid transformation [4] has gained a lot of

popularity as a tool for reducing the redundancy in raw images. The Laplacian pyramid with maximum selection rule was first introduced to model the binocular fusion in human stereo vision. The technique has also been applied for merging images from different modalities [14]. However, due to the lack of flexibility and blocking effects associated with the Laplacian pyramid technique interest shifted toward the utilization of the newly developed tool, the Wavelet Transforms.

Image fusion based on the wavelet transform has attracted many researchers. The development of the theory of multiresolution analysis [10] was the catalyst that made the wavelet transform accessible and an invaluable tool. The multispectral images provided by the sensors are decomposed using multiresolution analysis (decomposition) to an approximation and detail images at different levels. The decomposed approximation and details coefficient images carry information about the objects contained in the images but at different scale. Approximation images are fused together as well as detail images at same level then multiresolution reconstruction is used to generate the final fused image.

Image fusion can be accomplished using pixel level fusion, pixel neighborhood/area fusion, or feature based fusion. Pixel level fusion often tends to introduce noise and blurring effects in the fusion process. To overcome such a problem, area based and features based with elaborate construction of feature mapping and segmentation [13] has been utilized to fuse the coefficient images. In [5, 17], a human vision model was used to process the coefficient images before the fusion process.

In a study regarding the effect of quantizing the wavelet coefficients, it was found that such alteration produces visible artifacts in the reconstructed image [16]. Such visible noise is proportional to the amount of alteration of the coefficient and the impulse response of the filters used in the synthesis cascade. These visible artifacts have implications in applications that manipulate the wavelet coefficients such as in image fusion or compression of images.

The focus of this paper is to compare the results of pixel level and area level fusion on images that are corrupted with speckle like noise. The comparison will involve the fusion of raw images as well as their wavelet transform using five different techniques. The comparison is based on the visual perception of the fused images as well as their statistical properties using different fusing techniques.

2.1 Wavelet Transform of Images

Wavelet analysis has received wide acceptance as a new tool for signal and image processing. Wavelet analysis is capable of revealing aspects of data that other analysis techniques miss. It is capable of identifying trends, breakpoints, discontinuities in higher derivatives, and self-similarity [10, 13, 15].

In wavelet image processing, the multiresolution analysis is the most prevailing technique. It is commonly implemented using filter banks for decomposition and reconstruction as seen in figure 1 and 2 respectively. The low pass filter L and the high

pass filter H are designed to satisfy certain criteria such as perfect reconstruction and orthogonality. The process of decomposing an image to four coefficient images can be repeated using the approximation image ($L L$) at one level to generate a set of four coefficient images at a subsequent higher level. The net result is an image pyramid where the size of an image at one level is four times larger than that in a subsequently higher level. This is demonstrated in figure 3.

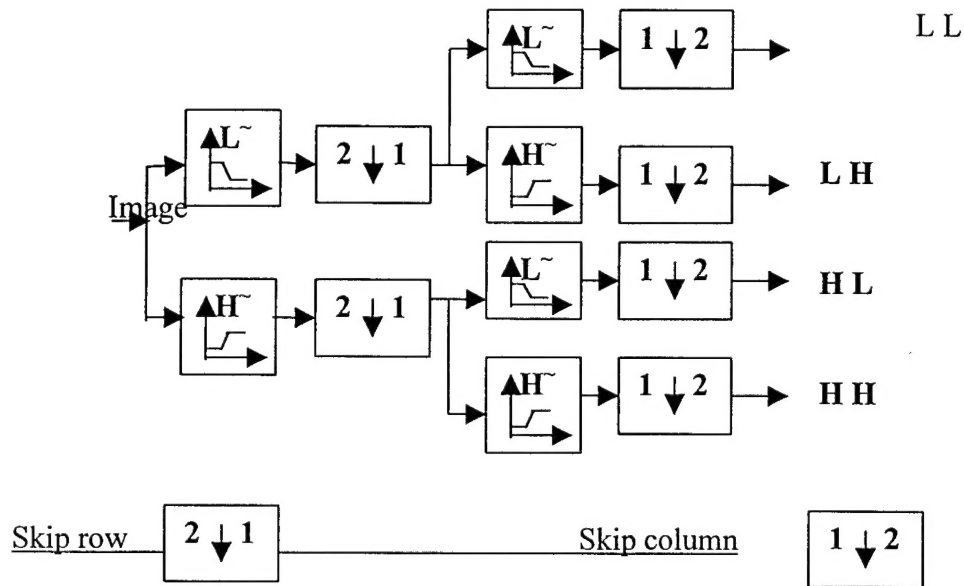
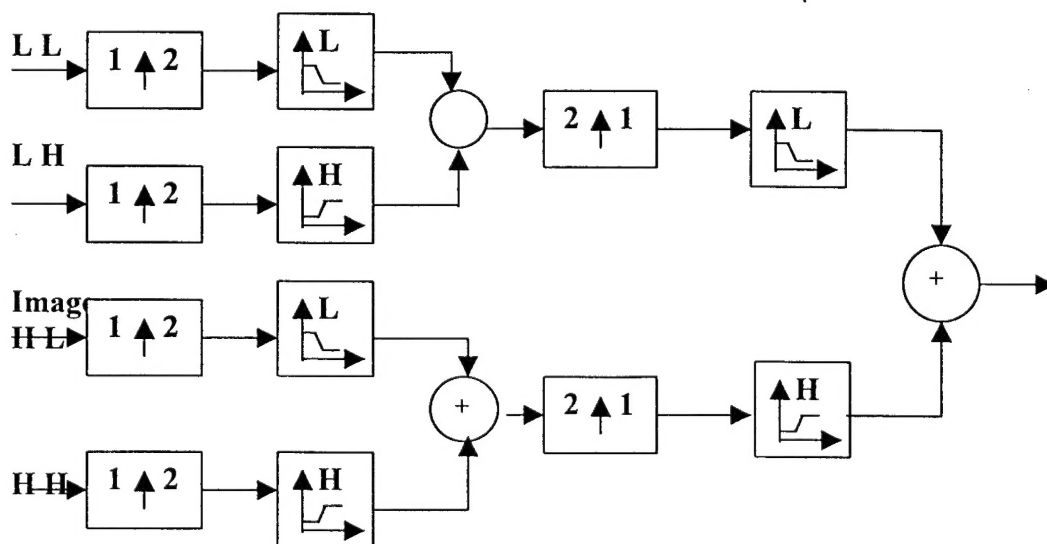
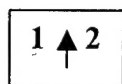


Figure 1, Wavelet image decomposition



Insert zero column



Insert zero row

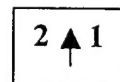


Figure 2, Wavelet image reconstruction

LL^3	LH^3	LH^2	LH^1
HL^3	HH^3		
HL^2		HH^2	
HL^1		HH^1	

Figure 3, Three levels of wavelet decomposition

Of special interest for implementing the low-pass and high-pass filters is the biorthogonal type of filters. They exhibit the property of linear phase that is a requirement for exact reconstruction of images [13].

3.0 EXPERIMENTAL RESULTS

To simulate the fusion of multispectral images, a color image is scanned and then decomposed into its three primary colors RGB images as shown in figure 4. The image size for those RGB images is 120x160 pixels. Those monochrome images are to be fused to a single monochrome image that should preserve all the prominent features in the three primary images. The decomposition was accomplished using the Matlab image processing toolbox function "TIFREAD". Table 1 presents the statistical properties (mean and standard deviation) of the RGB images. The reader's attention is directed toward the speckle noise like shown as dark dots around the edge of the balls.

The next step in the fusion process is the wavelet transformation of the RGB images. The Matlab wavelet toolbox function "DWT2" was utilized and the biorthogonal filters "BIOR3.7" were used for the decomposition and reconstruction of the images. Those filters are chosen for their perfect reconstruction capabilities among other attributes. Figures 5-7 present the wavelet coefficients images of the RGB images. The approximation image is a low pass filtered version of the corresponding image ($L L$ filtered image) while the horizontal details image ($L H$ filtered image) enhances features

parallel to the x-axis of the image. The vertical details image (H L filtered image) enhances the features parallel to the y-axis of the image while the diagonal details image (H H filtered image) emphasizes the features with diagonal characteristics.

3.1 Pixel level Fusion

The wavelet coefficients images of the RGB images are fused using pixel by pixel operations. For example, to generate the fused image from the coefficient images the maximum absolute value at each pixel position is chosen. That is, for example, the fused approximation image I_{af} is constructed by selecting the absolute maximum value at each pixel position from the three RGB approximation images (I_{ar} , I_{ag} , and I_{ab}).

$$I_{af}(i,j) = \text{Maximum} (|I_{ar}(i,j)|, |I_{ag}(i,j)|, |I_{ab}(i,j)|)$$

Similarly, the fused detail images are constructed. Figure 8 presents the fused wavelet coefficients of the RGB images. The fused wavelet coefficients images are then composed using the inverse wavelet transform (Matlab function IDWT2) to generate the fused image.

Another technique of generating a fused image is to use the average of wavelet coefficients at each pixel position. For example, the fused approximation image is generated using the following equation.

$$I_{af}(i,j) = \text{Average} (|I_{ar}(i,j)|, |I_{ag}(i,j)|, |I_{ab}(i,j)|)$$

Figure 9 presents the fused wavelet coefficients using the average pixel technique. In figure 10-a, the fused image based on maximum pixel value is presented while figure 10-b presents the fused image based on the average pixel value. Table 2 presents the statistics related to those two images.

3.2 Region Based Fusion

To take advantage of surrounding pixels, region based operations are utilized. A special 3x3 filter F is utilized to process the neighborhood pixels at each pixel position. In this case each coefficient image is processed using the filter prior to the fusion process. Thus, for example, the filtered approximation R image I_{arp} can be represented by,

$$I_{arp} = F * I_{ar}$$

The processed approximation and detail images are then merged to construct the fused image. One technique to utilize is using a filter that will measure the energy or support of the current pixel [6, 11]. Thus at each i,j pixel position, the pixel with the highest energy is selected to construct the fused wavelet coefficient images. Thus the fused approximation image is constructed from the processed RGB approximation images using the following equation,

$$I_{af}(i,j) = \text{Maximum} (|I_{arp}(i,j)|, |I_{agp}(i,j)|, |I_{abp}(i,j)|)$$

Figure 11 presents the fused coefficient images using the maximum pixel energy technique. Other filters can be designed to take advantage of the directional properties of the details images [6]. Such filter was utilized to compute the feature energy and the fused coefficient images are constructed as before and are presented in figure 12. The fused images using the above two techniques are presented in figure 13-a and figure 13-b respectively.

The filter F can also be designed to compute the statistical properties of the neighborhood around each pixel. Assuming normal distribution, the neighborhood mean $I(i,j)'$ and standard deviation $\sigma_{3 \times 3}$ can be computed. Then the fusion of the coefficient images can be implemented based on pooled statistics. Three different methods are utilized.

The pooled mean is computed and used to fuse the approximation and detail images of the RGB images. For example, to fuse the approximation images, the fused approximation image is computed as,

$$I_{af}(i,j) = (I_{ar}(i,j)' + I_{ag}(i,j)' + I_{ab}(i,j)') / 3.0$$

The detail images are fused in similar manner. Figure 14-a presents the fused image generated by the inverse wavelet transform of the fused approximation and detail images. The standard deviation $\sigma_{3 \times 3}$ at each pixel position is an indication of the gray level variability around each pixel and can be used as a weighting factor in the fusing processing of the approximation and detail images. In this case the fused approximation image would be computed as,

$$I_{af}(i,j) = \sigma_{ar3 \times 3} I_{ar}(i,j)' + \sigma_{ag3 \times 3} I_{ag}(i,j)' + \sigma_{ap3 \times 3} I_{ab}(i,j)'$$

Figure 14-b presents the fused image resulting from the above technique. Finally, the standard deviation of the entire image can also be used as a weighting factor for fusing the approximation and detail images. Thus the fused approximation image would be computed as,

$$I_{af}(i,j) = \sigma_{ar} I_{ar}(i,j)' + \sigma_{ag} I_{ag}(i,j)' + \sigma_{ap} I_{ab}(i,j)'$$

The fused image using this technique is presented in figure 14-c. Table 3 summarizes the statistical properties of the five fusion techniques as applied to wavelet based fusion.

For comparison purpose, the above five techniques for fusing images were applied using the raw RGB images. The fusion equations developed above were utilized to fuse the RGB images with results presented in figure 15 a-e. Table 4 summarizes the statistical properties of the fusion of the raw images.

4.0 DISCUSSIONS

Based on the utilization of those relatively simple fusion techniques and by visual inspection, it is apparent that fusing images corrupted with noise using the wavelet transform tends to enhance the appearance of the noisy regions. This is evident by comparing the original RGB images, and in particular the areas surrounding the speckles, to similar areas in the fused images. On the other hand fusing the raw RGB images did not show similar effect. In fact by comparing the $\sigma_{3 \times 3}$ weighted mean images, the edges are crispier in the fused raw RGB images than those in the wavelet based fused images. In addition, the statistical properties of raw fused images indicate a more effective edge enhancement as evident with low mean and small correlation values. In all other cases there is a consistent pattern of correlation between the fused images and the original RGB images.

This paper demonstrated that fusing the wavelet coefficients images directly can enhance the noise contents of the image. Unless additional efforts and computation in segmentation and feature extraction, a person is will advised to utilize the raw images as they provide better visual perception. It also indicates that simpler and more efficient segmentation algorithms are needed for pre fusion of wavelet coefficient images.

5.0 ACKNOWLEDGMENTS

This work was performed under the U.S. Navy Summer Faculty Research Program at the Naval Air Systems Command at Patuxanet River Station, MD. This program had been sponsored jointly by sponsored by the Department of the Navy and American Society for Engineering Education (ASEE) for whom the authors greatly appreciate their support.

6.0 REFERENCES

1. "Special Issue on Automatic Target Recognition", *IEEE Transactions on Image Processing*, Vol. 6, No. 1, January 1997.
2. "Special Issue on Automatic Target Recognition", *M.I.T., Lincoln Laboratory Journal*, Spring 1993, Vol 6, No. 1.
3. Brown, L. "A survey of Image Registration Techniques," *ACM Comput. Surv.* 24, 1992, pp. 325-376.
4. Burt, P. J. , "The Pyramid as Structure for Efficient Computation," in *Multiresolution Image Processing and Analysis*, pp. 6-35, Springer-Verlag, New York/Berlin, 1984.
5. Clark, J. J., and A. L. Yuille, 1990, *Data Fusion for Sensory Information Processing Systems*, Kluwer Academic Publishers, Boston.
6. Fukunaga, K., 1990, *Statistical Pattern Recognition*, Academic Press, 2nd Edition.
7. ,Li, H., Manjunath, B. S. ,and Mitra, S. K., "Multisensor Image Fusion using the Wavelet Transform," *Graphical Models and Image Processing*, Vol. 57, No. 3, May 1995, pp. 235-245.
8. Li, H., Manjunath, B. S. ,and Mitra, S. K., "A Contour Based Approach to Multisensor Image Registration," *IEEE Trans. Image Processing*, Vol.4, No. 3,

March 1995, pp. 320-334.

9. Luo, R., and M. Kay, 1992, "Data Fusion and Sensor registration: State-of-the-art in 1990s" In *Data Fusion in Robotics and Machine Intelligence*, edited by Abidi, M. and Gonzaloz, R., Eds., Academic Press, San Diego, pp.7-136.
10. Mallat, S.G., "A theory for Multiresolution Signal Decomposition: the Wavelet Representation," in *IEEE Trans. Pattern Analysis and Machine Intelligence*, Vol. PAM-11, July 1989, pp. 674-693.
11. Marr, D., and E. C. Hildreth, 1979, "Theory of Edge Detection", *M.I.T. Artificial Intelligence Laboratory Memo. No. 518, Cambridge, Mass., April*.
12. Singh, Ram-Nandan P., "An Intelligent Approach to Positive Target Identification", in *Soft Computing & Intelligent Systems*, (Editors, Sinha and Gupta), Academic Press, Chap. 22 (pp. 549-570), 1999.
13. Strang, Gilbert and Nguyen, Truong, *Wavelets and Filter Banks*, Wellesley-Cambridge Press, 1997.
14. Toet, A., Van Ruyven, ., L.J., and Valetton, J.M. "Merging Thermal and Visual Images by Contrast Pyramid," *Optical Engineering*, July 1989, Vol. 28, No. 7, pp. 789-792.
15. Xiaoyu Jiang, Liwei Zhou, Zhiyun Gao, " Multispectral Image Fusion Using Wavelet Transform," *SPIE* Vol. 2898, 1996, pp. 35-42.
16. Watson, Andrew B., Yang, Gloria Y., Solomon, Joshua A., and Villasenor, John, "Visibility of Wavelet Quantization Noise," *IEEE Transactions on Image Processing*, Vol. 6., No. 8, August 1997, pp. 1164-1175.
17. Wilson, A. T., S. K. Rogers, M. Kibrinski, 1997, "Perceptual-Based Image Fusion for Hyperspectral Data", *IEEE Trans. On Geoscience & Remote Sensing*, Vol. 35, No. 4, pp. 1007-1017, July.
18. Zelno, E.G., (Ed.), "Algorithms for Synthetic Aperture Radar Imagery IV", in *SPIE Vol. 3070, 1997*.

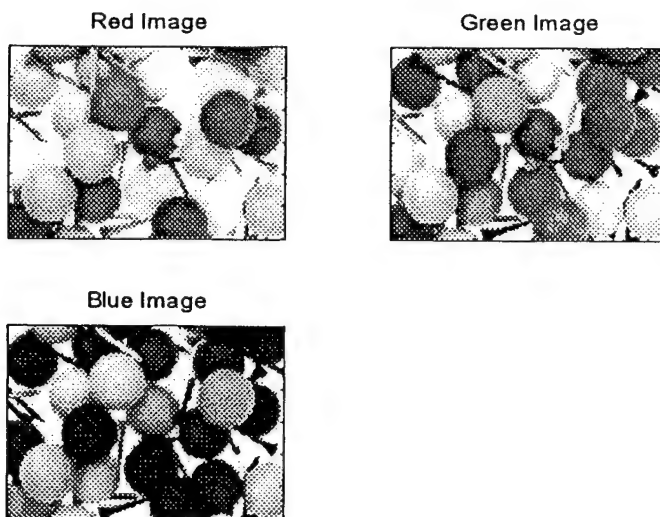


Figure 4

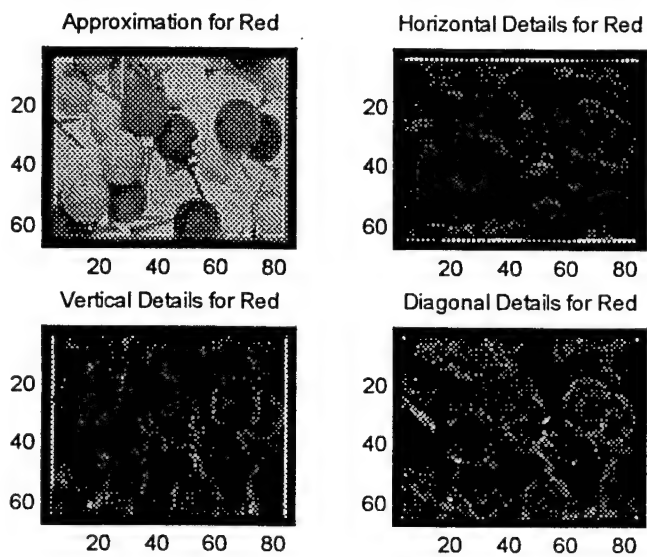


Figure 5

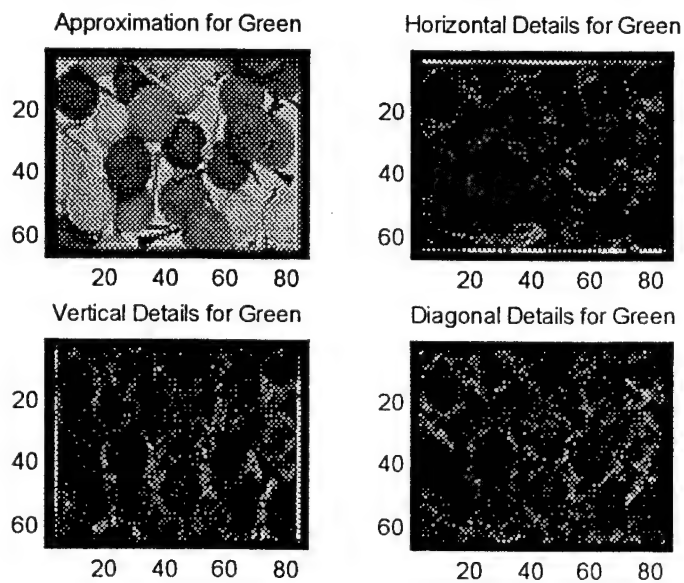


Figure 6

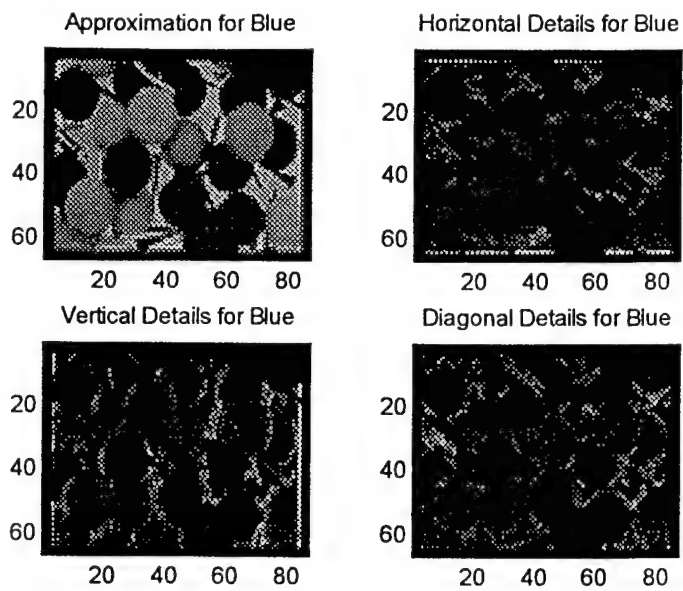


Figure 7

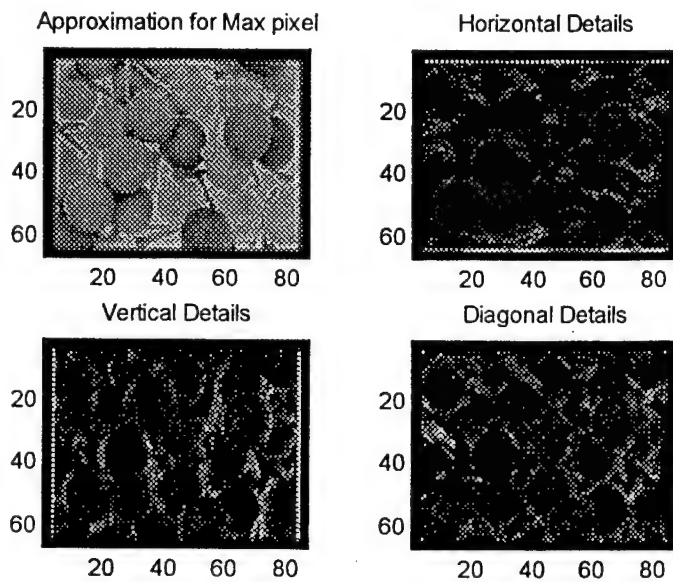


Figure 8

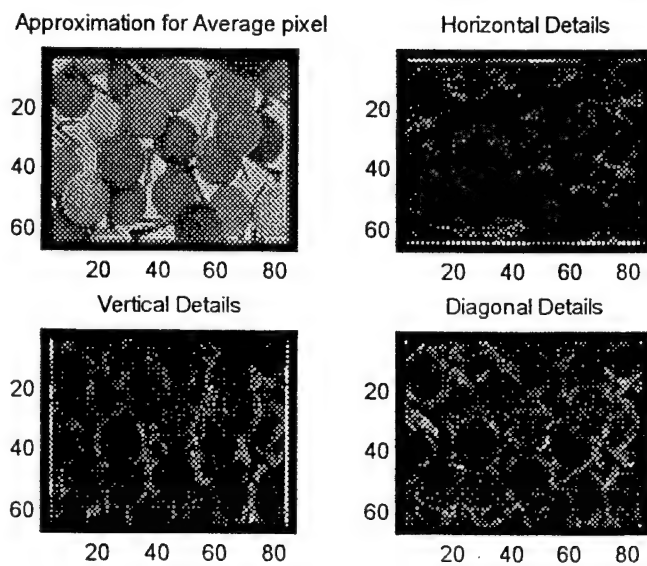
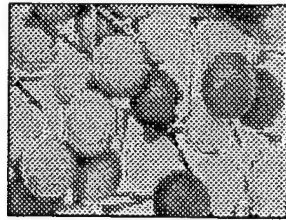


Figure 9

Max. abs. wavelet fused image



Average pixel wavelet fused image

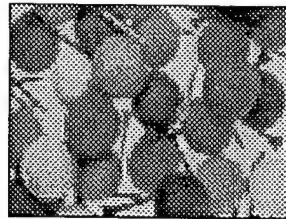
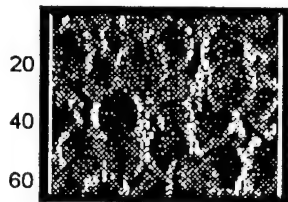


Figure 10

Approximation for Energy pixel



Vertical Details



Horizontal Details



Diagonal Details

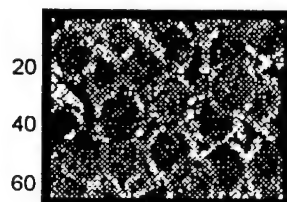


Figure 11

Approximation for feature Energy



Vertical Details



Horizontal Details



Diagonal Details

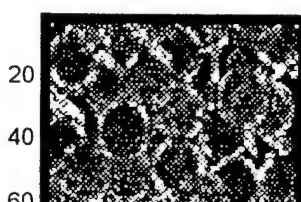
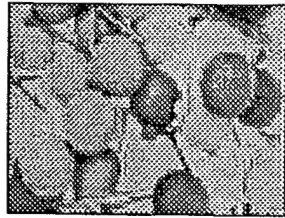
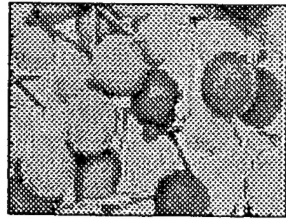


Figure 12

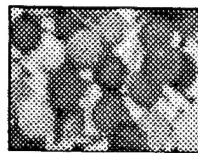
Energy fused image



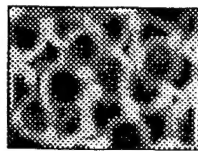
Feature fused image



Max. local mean Wavelet fused



Local St. Dev. weighted wavelet fused



Global St. Dev. weighted wavelet fused



Max. abs. pixel fused image, RGB Average pixel fused image, RGB



Max. energy fused image, RGB



Max. local meam, RGB



Local St. Dev. weighted, RGB



Global St. Dev. weighted, RGB



Figure 13

Figure 14

Figure 15

	R	G	B
Mean	0.715	0.562	0.437
Std. Dev.	0.298	0.331	0.376

Table 1, Statistics of the RGB images

	Pixel Maximum	Pixel Average
Mean	0.795	0.570
Std. Dev.	0.250	0.270
Correlation with Red	0.975	0.941
Correlation With Green	0.909	0.968
Correlation with Blue	0.790	0.891

Table 2, Statistics of pixel level based fusion of wavelet coefficients

	Pixel Energy	Feature Energy	Average mean	$\sigma_{3 \times 3}$ weighted mean	σ_{image} weighted mean
Mean	0.783	0.783	0.558	0.667	0.442
Std. Dev.	0.246	0.245	0.232	0.472	0.183
Correlation with Red	0.974	0.975	0.945	0.819	0.945
Correlation With Green	0.906	0.907	0.960	0.829	0.961
Correlation with Blue	0.785	0.785	0.874	0.769	0.876

Table 3, Statistics for fusion of wavelet coefficients based on a 3x3 window

	Pixel Maximum	Pixel Average
Mean	0.790	0.571
Std. Dev.	0.231	0.269
Correlation with Red	0.983	0.946
Correlation With Green	0.916	0.979
Correlation with Blue	0.796	0.908

Table 4, Statistics of pixel level fusion of RGB images

	Pixel Energy	Average mean	$\sigma_{3 \times 3}$ weighted mean	σ_{image} weighted mean
Mean	0.789	0.565	0.124	0.557
Std. Dev.	0.232	0.251	0.171	0.256
Correlation with Red	0.983	0.947	0.595	0.938
Correlation With Green	0.916	0.972	0.615	0.972
Correlation with Blue	0.796	0.894	0.582	0.906

Table 5, Statistics for fusion of raw RGB images based on a 3x3 window

REPORT DOCUMENTATION PAGE				Form Approved OMB No. 0704-0188	
Public reporting burden for this collection of information is estimated to average 1 hour per response, including the time for reviewing instructions, searching existing data sources, gathering and maintaining the data needed, and completing and reviewing this collection of information. Send comments regarding this burden estimate or any other aspect of this collection of information, including suggestions for reducing this burden, to Department of Defense, Washington Headquarters Services, Directorate for Information Operations and Reports (0704-0188), 1215 Jefferson Davis Highway, Suite 1204, Arlington, VA 22202-4302. Respondents should be aware that notwithstanding any other provision of law, no person shall be subject to any penalty for failing to comply with a collection of information if it does not display a currently valid OMB control number. PLEASE DO NOT RETURN YOUR FORM TO THE ABOVE ADDRESS.					
1. REPORT DATE		2. REPORT TYPE Professional Paper		3. DATES COVERED	
4. TITLE AND SUBTITLE Image-Based Automatic Target Recognition				5a. CONTRACT NUMBER	
				5b. GRANT NUMBER	
				5c. PROGRAM ELEMENT NUMBER	
6. AUTHOR(S) Dr. Ram Nandan P. Singh Professor Mahmoud A. Abdallah				5d. PROJECT NUMBER	
				5e. TASK NUMBER	
				5f. WORK UNIT NUMBER	
7. PERFORMING ORGANIZATION NAME(S) AND ADDRESS(ES) Naval Air Warfare Center Aircraft Division 22347 Cedar Point Road, Unit #6 Patuxent River, Maryland 20670-1161				8. PERFORMING ORGANIZATION REPORT NUMBER	
9. SPONSORING/MONITORING AGENCY NAME(S) AND ADDRESS(ES) Naval Air Systems Command 47123 Buse Road Unit IPT Patuxent River, Maryland 20670-1547				10. SPONSOR/MONITOR'S ACRONYM(S)	
				11. SPONSOR/MONITOR'S REPORT NUMBER(S)	
12. DISTRIBUTION/AVAILABILITY STATEMENT Approved for public release; distribution is unlimited.					
13. SUPPLEMENTARY NOTES					
14. ABSTRACT An image-based automatic target recognition (IATR) is basically a tactical decision aid that integrates all of the available information and produces a dynamic composite picture of a target for visualization and evaluation by an operator. In modern warfare, it has become an indispensable tool for precision strikes and surveillance missions of defense weapon systems. An IATR processes imagery data received from diverse imaging sensors for the purpose of target detection and recognition in real time. Using Wavelet Transforms, images are fused at different resolution levels to obtain a fused image. It has also been demonstrated that fusing the wavelet coefficient images directly can enhance the recognition contents of the image. This composite image contains all the information of interest for an IATR. In addition, an evaluation methodology based on visual perception and on statistical properties of the fused image is presented.					
15. SUBJECT TERMS					
16. SECURITY CLASSIFICATION OF:			17. LIMITATION OF ABSTRACT	18. NUMBER OF PAGES	19a. NAME OF RESPONSIBLE PERSON
a. REPORT	b. ABSTRACT	c. THIS PAGE			Dr. Ram Nandan P. Singh
Unclassified	Unclassified	Unclassified	Unclassified	16	19b. TELEPHONE NUMBER (include area code) (301) 342-2316

Standard Form 298 (Rev. 8-98)
Prescribed by ANSI Std. Z39-18

DRUG QUALITY IMPROVED 4